

Article

## Permeation of Light Gases through Hexagonal Ice

Joana Durão <sup>1</sup> and Luis Gales <sup>1,2,\*</sup>

<sup>1</sup> IBMC—Institute for Molecular and Cell Biology, University of Porto Porto, Rua do Campo Alegre 823, Porto 4150-180, Portugal; E-Mail: joana.oliveira@gmail.com

<sup>2</sup> ICBAS—Institute of Biomedical Sciences Abel Salazar, Porto 4099-003, Portugal

\* Author to whom correspondence should be addressed; E-Mail: lgales@ibmc.up.pt; Tel.: +351-222-062-200. Fax: +351-222-062-232.

Received: 16 July 2012; in revised form: 21 August 2012 / Accepted: 27 August 2012 /

Published: 5 September 2012

---

**Abstract:** Gas separation using porous solids have attracted great attention due to their energetic applications. There is an enormous economic and environmental interest in the development of improved technologies for relevant processes, such as H<sub>2</sub> production, CO<sub>2</sub> separation or O<sub>2</sub> and N<sub>2</sub> purification from air. New materials are needed for achieving major improvements. Crystalline materials, displaying unidirectional and single-sized pores, preferentially with low pore tortuosity and high pore density, are promising candidates for membrane synthesis. Herein, we study hexagonal ice crystals as an example of this class of materials. By slowly growing ice crystals inside capillary tubes we were able to measure the permeation of several gas species through ice crystals and investigate its relation with both the size of the guest molecules and temperature of the crystal.

**Keywords:** ice; light gases; diffusion

---

### 1. Introduction

Separation or purification of light gases is crucial in many industrial activities. In fact, there is an enormous economic and environmental interest in the development of better technologies for relevant processes such as H<sub>2</sub> production, CO<sub>2</sub> separation or O<sub>2</sub> and N<sub>2</sub> purification from air. Membrane separation is growing as a low-cost and energy-efficient alternative to traditional methods, such as adsorption or cryo-separation. Most membranes in use in industry are polymeric [1], and despite the ongoing development of better polymeric materials, there is a trade-off between flow rates and

selectivities [2]. Crystalline materials, displaying unidirectional and single-sized pores are promising candidates for membrane synthesis. Metal-organic frameworks (MOFs) [3,4] and peptide supramolecular systems [5–8] are among the most promising crystal structures, due to the variety of pore sizes and high pore density. Nevertheless, the key challenge in the context of using crystalline materials is to scale up the fabrication techniques of either dense polycrystalline layers [3] or mixed matrix membranes, which embed the selective particles inside the polymeric matrix [4].

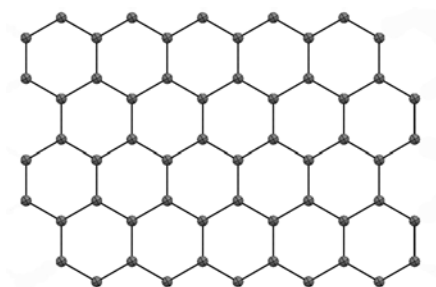
It is well known that ordinary water and several organic compounds [9] solidify in a regular geometric lattice (crystal) containing unidirectional nanochannels. Here, using water ice as a model, we demonstrate that under controlled phase transition conditions it is possible to induce the orientation of the crystal lattice inside capillary tubes: a process that may find very interesting applications. We show that, inside capillary tubes, hexagonal ice crystals form by slowly growing in the direction of the *c*-axis and that they can be used as single crystal membranes able to distinguish between different gas molecules. We observed that the gas molecules cannot escape through the ice-glass capillary wall interface, which enables an easy scale-up by simply using perforated solid plates to promote multiple crystal growth. Moreover, we found that the flow rate of the gas species is severely regulated by ice temperature, expanding the number of potential species that may be separated.

## 2. Experimental

### 2.1. Crystallization

The crystallization of ultrapure water was achieved inside capillaries of variable diameters (from 2.0 mm to 0.1 mm) and applying different temperature decreasing rates. The ice crystal structures and the alignment of the *c*-axis relative to the capillary were determined by X-ray diffraction (see Supplementary Information). We obtained the well-known ice I<sub>h</sub> hexagonal crystal structure [10] with an oxygen atom on each vertex (Figure 1). The crystal disorder decreased (better-diffracting crystals) when using thinner capillaries and lower cooling rates (10 K/hr down to 260 K followed by 360 K/hr until reaching the required temperature). It is worth pointing out that although the freezing process often resulted in disordered ice, the crystallographic *c*-axis was always coincident with the capillary axis in the well-diffracting crystals.

**Figure 1.** Crystal structure of ice I<sub>h</sub> at 150 K viewed along the *c*-axis. Hydrogen atoms are not shown.



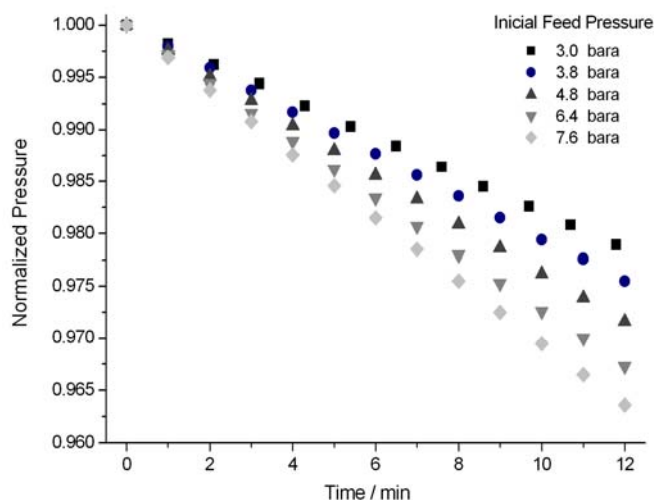
## 2.2. Single-Crystal Permeation Experiments

Single-crystal permeation experiments were performed against the atmosphere using a pressurized feed gas chamber (see the scheme in the Supplementary Information). A small volume (around  $7 \times 10^{-3}$   $\mu\text{L}$ ) of ultrapure water (milli-Q water) was introduced inside a glass capillary. The ice crystal was obtained by cooling at temperature rate of 10 K/hr until 260 K followed by 360 K/hr towards the predetermined temperature. A standard cryostream cooler for X-ray diffraction was used. Pressure of the feed gas chamber was monitored and permeabilities were determined through a mass balance on the chamber volume.

## 3. Results and Discussion

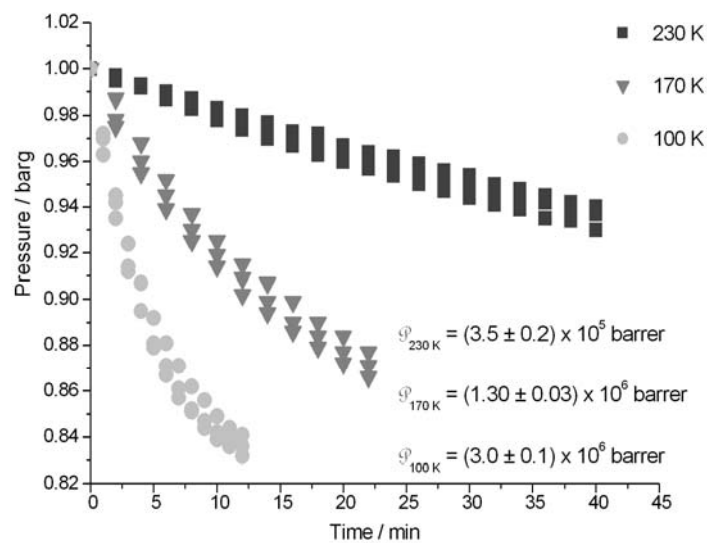
We measured ice permeability towards helium (Figure 2), the molecule with the smallest kinetic diameter (2.6 Å), and found that it is permeable in the *c*-axis direction. Disordered ice crystals were non-permeable. The hexagonal ice void nanochannels are smaller than all the gas molecular dimensions, including helium (see Supplementary Information). However, the unexpected penetration of small molecules through other hydrogen-bonded supramolecular crystals was already observed and was attributed to the flexibility of the crystal framework [7,11].

**Figure 2.** Feed pressure drop normalized by the pressure gradient across the ice crystal.



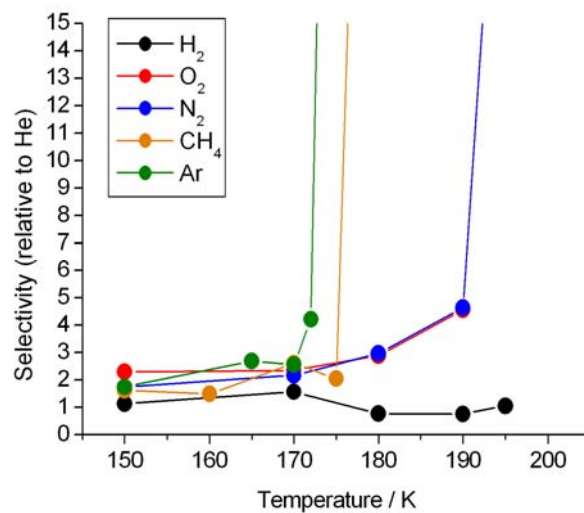
The increase in the pressure gradient across the ice crystals predictably enhances the helium flow rate (Figure 2). However, the helium flow rate diminishes significantly with increasing temperature, which is not expected in diffusion processes, such as diffusion of trace gases in hexagonal ice [12,13]. This behavior may be associated with a temperature effect in the stability of the ice crystal phase (Figure 3).

**Figure 3.** Temperature effect of the ice  $I_h$  permeability towards helium. Pressure drop in the feed gas chamber.



We then studied the permeation of other gas compounds through ice (Figure 4). Interestingly the flow rate diminishes with increasing temperature until a critical value is reached, above which the compound does not permeate.

**Figure 4.** Ice  $I_h$  selectivity of argon, methane, nitrogen, oxygen and hydrogen, relative to helium.



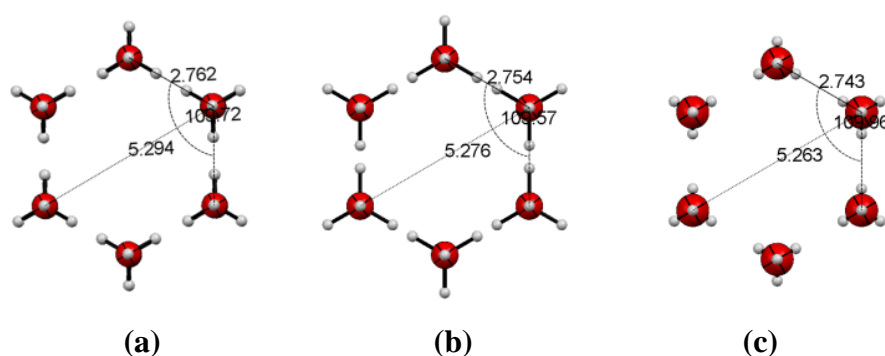
Almost all binary combinations of gas species investigated can be potentially separated at a certain temperature. Oxygen and nitrogen, however, present an overlapping exclusion temperature, whereas the helium/hydrogen pair involves critical temperatures above the studied range. The critical temperatures do not correlate completely with the kinetic diameters of the gas species (Table 1).

**Table 1.** Kinetic diameters and excluding temperatures of the gas compounds.

Gas	Kinetic diameters (Å)	Gas excluding temperature (K)
Helium	2.60	>195 K
Hydrogen	2.89	>195 K
Oxygen	3.46	195 K
Nitrogen	3.64	195 K
Methane	3.80	180 K
Argon	3.40	175 K

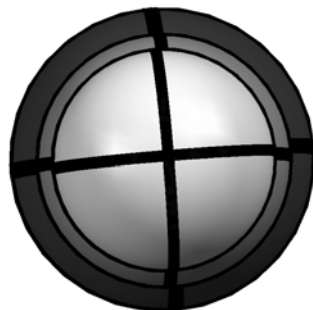
Anisotropic molecules seem to behave as being slightly “smaller” than expected from the kinetic diameters, probably because they become partially aligned inside the nanochannels. We have already observed this behavior in the permeation through dipeptide microporous crystals [7].

In addition, we also investigated the temperature effect on ice structure by single-crystal X-ray diffraction. It has already been observed that above 100 K there is a residual thermal expansion, virtually isotropic, of powdered ice  $I_h$ . [14] Hexagonal ice confined to 0.1 mm capillary tubes exhibits, in the 150–240 K temperature range, a slight decrease in the  $a$  crystal lattice (4.5167(15) Å @150 K to 4.492(4) Å @240 K, uncertainties in parenthesis) and an increase in the  $c$  crystal lattice (7.290(3) Å @150 K to 7.335(7) Å @240 K). Overall, there is a negative thermal expansion of the cell volume (128.79(8) Å<sup>3</sup> @150 K to 128.16(19) Å<sup>3</sup> @240 K) as it was formerly obtained by Dantl (1962) by single crystal experiments [15]. Accordingly, there is a small contraction of the hexagonal ice rings which can hardly explain the magnitude of the temperature effect in the gas flow rates (Figure 5).

**Figure 5.** Ice  $I_h$  hexagonal ring dimensions at (a) 150 K; (b) 195 K; and (c) 240 K.

The increase in thermal motion of the oxygen atoms is probably more decisive. Figure 6 shows the thermal ellipsoids of the oxygen atoms at 150 K, 195 K and 240 K of ice formed inside 0.1 mm capillaries. High-resolution neutron diffraction studies of ice  $I_h$  had already shown an increase in the average thermal displacement of O atoms from 0.118 Å @66 K to 0.208 Å @223 K rmsd [16]. The increase with temperature of O thermal motion is also correlated with a decrease of the ice crystal structure stability. It is possible that when reaching a given temperature, the gas molecules interact with the ice structure, blocking the flow through. However, we checked that the flux is re-established after replacing a non-permeating gas by helium.

**Figure 6.** Thermal ellipsoids of the oxygen atoms of ice  $I_h$  crystal structures formed inside 0.1 mm capillaries at 150 K, 195 K and 240 K (from light to dark grey respectively). The three ellipsoids are shown at the same probability level.



The mass transport through the ice structure is considerably fast. The helium flow rate through the hexagonal ice columns is approximately as fast as the flux through the permanent nanochannels of the L-valyl-L-isoleucine (VI) crystals [7]. The estimated VI nanochannels diameter stands between 3.0 and 3.7 Å depending on the determination method [11]. The high flow rates through the channels reflect the negligible tortuosity of the hexagonal columns and the high flexibility of the ice framework. In addition to this, the almost unbeatable pore density of the  $I_h$  crystalline form results in very high permeabilities.

Ice phase transitions and ice–gas interactions (gas hydrate stability and gas diffusion mechanisms) are deeply investigated but poorly understood. Nevertheless, our results are intriguing in light of the global perspective in the field.

The ice  $I_c$ –ice  $I_h$  transition temperature is located between 160 K and 205 K [17] and the reasons behind such variability are not yet clear. However we are confident, based on the X-ray diffraction data, that by slowly decreasing the temperature of water inside capillary tubes at atmospheric pressure, the hexagonal form is maintained down to 150 K.

Gas molecules with molecular dimension lower than 0.9 nm can be incorporated in water crystalline inclusions—known as clathrate hydrates. Most hydrates belong to three structural families, two cubic forms and one hexagonal form [18–21]. All the gas species used in this work are described as being among the ones known to form clathrate-like structures [17,22,23]. The mechanism of dissociation of clathrate hydrates is still not well understood. Some clathrate hydrates show a self-preservation behavior, even outside the zone of thermodynamic stability of the hydrate, that is dependent on the type of the guest molecule [22–25]. Guest molecules can impose variations in the lattice constants of the hydrate structure and induce a significant weakening of the host structure [26]. Temperature transition to a non-permeable behavior towards gases is very drastic (Figure 4). As mentioned above, this may be related to the formation of a new ice phase where the guest molecules become trapped. A similar mechanism was already proposed to the dissociation behavior of clathrate hydrates in the 180–220 K range [20]. Unfortunately, diffusion measurements of trace gases in ice are scarce and sometimes contradictory. Molecular dynamics simulation studies are more frequent but the understanding of the diffusion mechanisms remains poorly understood. Ikeda-Fukazawa *et al.* [27–29] argued that small apolar guest molecule, such as He, Ne, Ar or  $H_2$ , diffuse without distorting the ice lattice while large molecules, such as

O<sub>2</sub>, N<sub>2</sub>, CO<sub>2</sub> and CH<sub>4</sub>, diffuse by a bond-breaking mechanism. However, Demurov and colleagues [30] reported molecular dynamic simulations of CO<sub>2</sub> through defect-free hexagonal ice at 200 K and observed no evidence of diffusion. Alavi and Ripmeester [22] on the other hand showed that H<sub>2</sub> can diffuse out of the hydrates through the hexagonal rings, or even through the smaller pentagonal rings. Mitlin *et al.* [31] argued that Xe can easily penetrate the ice hexagonal structure by a mechanism of adsorption and induced crystal disorder. Peters *et al.* [32] observed that methane does not fit through the six membered ring without distortion, so one hydrogen bond in the water ring must break at a transition state. Ballenegger and colleagues [33] showed that formaldehyde diffuses predominantly through a bond-breaking mechanism of the ice structure.

Here we show that H<sub>2</sub>, O<sub>2</sub>, N<sub>2</sub>, CH<sub>4</sub> and Ar can diffuse through the hexagonal ice structure. Diffusion of these compounds was already predicted theoretically by other authors [34]. However, we cannot ascertain whether defects in the crystal matrix or local disorder induced by guest species are relevant or not for the diffusion mechanism. We tried to obtain gas sorption equilibrium data to corroborate our findings but without success. The hexagonal ice sample size (around  $7 \times 10^{-3}$  μL) is too small to measure gas sorption uptake. Nevertheless, adsorption isotherms of light gases, such as H<sub>2</sub>, N<sub>2</sub> and CO<sub>2</sub> in hexagonal ice, were already reported in the literature [35,36].

#### 4. Conclusions

Ice was already used as a chromatographic stationary phase to separate enantiomers [37]. Here, we have shown that hexagonal ice may be used as a molecular sieve to separate light gases with commercial value. Despite the high selectivities and permeabilities, the practical use of ice for gas separations is certainly limited by low stability of the ice structure and low operating temperatures. Nevertheless, our results have a long-term interest as they will motivate the search for other compounds that solidify at higher temperatures into similar but more stable crystalline structures. The possibility of easy scale-up into polycrystalline membranes with exceptional performance certainly looks very promising.

#### Acknowledgments

This work was supported by Fundação para a Ciência e Tecnologia (project PTDC/CTM/64191/2006) and by a PhD scholarship to Joana Durão (SFRH/BD/69960/2010).

#### References

1. Bernardo, P.; Drioli, E.; Golemme, G. Membrane gas separation: A review/state of the art. *Ind. Eng. Chem. Res.* **2009**, *48*, 4638–4663.
2. Robeson, L.M. The upper bound revisited. *J. Membr. Sci.* **2008**, *320*, 390–400.
3. Bux, H.; Liang, F.; Li, Y.; Cravillon, J.; Wiebcke, M.; Caro, J. Zeolitic imidazolate framework membrane with molecular sieving properties by microwave-assisted solvothermal synthesis. *J. Am. Chem. Soc.* **2009**, *131*, 16000–16001.
4. Bae, T.H.; Lee, J.S.; Qiu, W.; Koros, W.J.; Jones, C.W.; Nair, S. A high-performance gas-separation membrane containing submicrometer-sized metal-organic framework crystals. *Angew. Chem. Int. Ed.* **2010**, *49*, 9863–9866.

5. Soldatov, D.V.; Moudrakovski, I.L.; Ripmeester, J.A. Dipeptides as microporous materials. *Angew. Chem. Int. Ed.* **2004**, *43*, 6308–6311.
6. Comotti, A.; Bracco, S.; Distefano, G.; Sozzani, P. Methane, carbon dioxide and hydrogen storage in nanoporous dipeptide-based materials. *Chem. Commun.* **2009**, *3*, 284–286.
7. Afonso, R.V.; Durão, J.; Mendes, A.; Damas, A.M.; Gales, L. Dipeptide crystals as excellent permselective materials: Sequential exclusion of argon, nitrogen, and oxygen. *Angew. Chem. Int. Ed.* **2010**, *49*, 3034–3036.
8. Afonso, R.; Mendes, A.; Gales, L. Peptide-based solids: Porosity and zeolitic behavior. *J. Mater. Chem.* **2012**, *22*, 1709–1723.
9. Kameta, N.; Minamikawa, H.; Masuda, M. Supramolecular organic nanotubes: How to utilize the inner nanospace and the outer space. *Soft Matter* **2011**, *7*, 4539–4561.
10. Pauling, L. The Structure and entropy of ice and of other crystals with some randomness of atomic arrangement. *J. Am. Chem. Soc.* **1935**, *57*, 2680–2684.
11. Soldatov, D.V.; Moudrakovski, I.L.; Grachev, E.V.; Ripmeester, J.A. Micropores in crystalline dipeptides as seen from the crystal structure, the pycnometry, and  $^{129}\text{Xe}$  NMR spectroscopy. *J. Am. Chem. Soc.* **2006**, *128*, 6737–6744.
12. Geil, B.; Kirschgen, T.M.; Fujara, F. Mechanism of proton transport in hexagonal ice. *Phys. Rev. B* **2005**, *72*, 014304:1–014304:10.
13. Markland, T.E.; Manolopoulos, D.E. An efficient ring polymer contraction scheme for imaginary time path integral simulations. *J. Chem. Phys.* **2008**, *129*, 074501:1–074501:8.
14. Rottger, K.; Endriss, A.; Ihringer, J.; Doyle, S.; Kuhs, W.F. Lattice constants and thermal expansion of  $\text{H}_2\text{O}$  and  $\text{D}_2\text{O}$  ice Ih between 10 and 265 K. *Acta Crystallogr. Sect. B* **1994**, *50*, 644–648.
15. Dantl, G. Wärmeausdehnung von  $\text{H}_2\text{O}$ - und  $\text{D}_2\text{O}$ -einkristallen (In German). *Z. Phys.* **1962**, *166*, 115–118.
16. Kuhs, W.F.; Lehmann, M.S. The structure of ice Ih by neutron diffraction. *J. Phys. Chem.* **1983**, *87*, 4312–4313.
17. Kuhs, W.F.; Genov, G.; Staykova, D.K.; Hansen, T. Ice perfection and onset of anomalous preservation of gas hydrates. *Phys. Chem. Chem. Phys.* **2004**, *6*, 4917–4920.
18. Jeffrey, G.A. *Comprehensive Supramolecular Chemistry*; Atwood, J.L., Davies, J.E.D., MacNicol, D.D., Vogtle, F., Lehn, J.M., Eds.; Pergamon: New York, NY, USA, 1996.
19. Ripmeester, J.A.; Tse, J.S.; Ratcliffe, C.I.; Powell, B.M. A new clathrate hydrate structure. *Nature* **1987**, *325*, 135–136.
20. Udachin, K.A.; Ratcliffe, C.I.; Enright, G.D.; Ripmeester, J.A. Structure H hydrate: A single crystal diffraction study of 2,2-dimethylpentane-5(Xe,  $\text{H}_2\text{S}$ )- $34\text{H}_2\text{O}$ . *Supramol. Chem.* **1997**, *8*, 173–176.
21. Lu, H.; Seo, Y.T.; Lee, J.W.; Moudrakovski, I.; Ripmeester, J.A.; Chapman, N.R.; Coffin, R.B.; Gardner, G.; Pohlman, J. Complex gas hydrate from the Cascadia margin. *Nature* **2007**, *445*, 303–306.
22. Alavi, S.; Ripmeester, J.A. Hydrogen-gas migration through clathrate hydrate cages. *Angew. Chem. Int. Ed.* **2007**, *46*, 6102–6105.

23. Takeya, S.; Ripmeester, J.A. Dissociation behavior of clathrate hydrates to ice and dependence on guest molecules. *Angew. Chem. Int. Ed.* **2008**, *47*, 1276–1279.
24. Fray, N.; Marboeuf, U.; Brissaud, O.; Schmitt, B. Equilibrium data of methane, carbon dioxide, and xenon clathrate hydrates below the freezing point of water. Applications to astrophysical environments. *J. Chem. Eng. Data* **2010**, *55*, 5101–5108.
25. Strobel, T.A.; Somayazulu, M.; Hemley, R.J. Phase behavior of H<sub>2</sub> + H<sub>2</sub>O at high pressures and low temperatures. *J. Phys. Chem. C* **2011**, *115*, 4898–4903.
26. Buch, V.; Devlin, J.P.; Monreal, I.A.; Jagoda-Cwiklik, B.; Uras-Aytemiz, N.; Cwiklik, L. Clathrate hydrates with hydrogen-bonding guests. *Phys. Chem. Chem. Phys.* **2009**, *11*, 10245–10265.
27. Ikeda-Fukazawa, T.; Horikawa, S.; Hondoh, T.; Kawamura, K. Molecular dynamics studies of molecular diffusion in ice Ih. *J. Chem. Phys.* **2002**, *117*, 3886–3896.
28. Ikeda-Fukazawa, T.; Kawamura, K.; Hondoh, T. Diffusion of nitrogen gas in ice Ih. *Chem. Phys. Lett.* **2004**, *385*, 467–471.
29. Ikeda-Fukazawa, T.; Kawamura, K.; Hondoh, T. Mechanism of molecular diffusion in ice crystals. *Mol. Simulat.* **2004**, *30*, 973–979.
30. Demurov, A.; Radhakrishnan, R.; Trout, B.L. Computations of diffusivities in ice and CO<sub>2</sub> clathrate hydrates via molecular dynamics and Monte Carlo simulations. *J. Chem. Phys.* **2002**, *116*, 702–709.
31. Mitlin, S.; Lemak, A.S.; Torrie, B.H.; Leung, K.T. Surface adsorption and trapping of Xe on hexagonal ice at 180 K by molecular dynamics simulations. *J. Phys. Chem. B* **2003**, *107*, 9958–9963.
32. Peters, B.; Zimmermann, N.E.R.; Beckham, G.T.; Tester, J.W.; Trout, B.L. Path sampling calculation of methane diffusivity in natural gas hydrates from a water-vacancy assisted mechanism. *J. Am. Chem. Soc.* **2008**, *130*, 17342–17350.
33. Ballenegger, V.; Picaud, S.; Toubin, C. Molecular dynamics study of diffusion of formaldehyde in ice. *Chem. Phys. Lett.* **2006**, *432*, 78–83.
34. Hori, A.; Hondoh, T. Theoretical study on the diffusion of gases in hexagonal ice by the molecular orbital method. *Can. J. Phys.* **2003**, *81*, 251–259.
35. Ocampo, J.; Klinger, J. Adsorption of N<sub>2</sub> and CO<sub>2</sub> on ice. *J. Colloid Interface Sci.* **1982**, *86*, 377–383.
36. Pascal, T.A.; Boxe, C.; Goddard, W.A. An inexpensive, widely available material for 4 wt% reversible hydrogen storage near room temperature. *J. Phys. Chem. Lett.* **2011**, *2*, 1417–1420.
37. Shamoto, T.; Tasaki, Y.; Okada, T. Chiral ice chromatography. *J. Am. Chem. Soc.* **2010**, *132*, 13135–13137.